

# **TWIST1 Expression in Breast Cancer Cells Facilitates Bone Metastasis Formation**

Martine Croset,<sup>1,3,4</sup> Delphine Goehrig,<sup>1,3,4</sup> Agnieszka Frackowiak,<sup>1,3,4</sup> Edith Bonnelye,<sup>1,3,4</sup> Stéphane Ansieau,<sup>2,3,4,5,6,7</sup> Alain Puisieux,<sup>2,3,4,5,6,7</sup> and Philippe Clézardin<sup>1,3,4</sup>

<sup>1</sup>INSERM, UMR\_S1033, Lyon, France

<sup>2</sup>INSERM, UMR\_S1052, Centre de Recherche en Cancérologie de Lyon, Lyon, France

<sup>3</sup>University of Lyon, Villeurbanne, France

<sup>4</sup>LabEx DEVweCAN, Lyon, France

<sup>5</sup>Centre Léon Bérard, Lyon, France

<sup>6</sup>UNIV UMR1052, Centre de Recherche en Cancérologie de Lyon, Lyon, France

<sup>7</sup>Institut Universitaire de France, Paris, France

## **ABSTRACT**

The transcription factor TWIST1 induces epithelial-mesenchymal transition and/or escape to the oncogenic-induced failsafe program, facilitating the intravasation of breast cancer cells in the systemic circulation and their dissemination to the lungs. Its involvement in breast cancer bone metastasis is unknown. To address this question, human osteotropic MDA-MB-231/B02 breast cancer cells were stably transfected with a Tet-inducible vector encoding for *TWIST1*, whose expression was specifically repressed in the presence of doxycycline (dox). The intra-arterial inoculation of transfectants expressing *TWIST1* in immunodeficient mice substantially increased the extent of osteolytic lesions in these animals, being 50% larger than that of animals bearing mock-transfected tumors, as determined by radiography. This difference was accompanied by a sharp reduction of the bone volume (indicating a higher bone destruction) and a twofold increase in the tumor volume compared with mice bearing mock-transfected tumors, as determined by histomorphometry. Importantly, the suppression of *TWIST1* expression in MDA-MB-231/B02 cells in the presence of dox abolished the stimulatory effect of *TWIST1* on bone metastasis formation in vivo. Additionally, examination of the bone marrow from untreated and dox-treated animals on day 7 after tumor cell inoculation, at which time there was no evidence of radiographic osteolytic lesions, revealed that the number of tumor cell colonies that were recovered from the bone marrow of untreated mice was dramatically increased compared with that of dox-fed animals. In vitro, *TWIST1* expression promoted tumor cell invasion and enhanced microRNA 10b (miR-10b) expression, a proinvasive factor, but was dispensable for growth of tumor cells. In vivo, the repression of miR-10b substantially decreased the presence of *TWIST1*-expressing breast cancer cells in the bone marrow. Overall, these results establish that *TWIST1* facilitates breast cancer bone metastasis formation through a mechanism dependent of miR-10b, which leads to increase tumor burden and bone destruction. © 2014 American Society for Bone and Mineral Research.

**KEY WORDS:** TWIST1; BONE; METASTASIS; BREAST CANCER; MIR-10B; INVASION

## **Introduction**

Breast cancer is prone to metastasize to bone: around 70% to 80% of patients with advanced disease exhibit osteolytic bone metastases.<sup>(1)</sup> Once metastatic breast cancer cells are in the bone marrow, they cannot destroy bone on their own. Instead, they alter the functions of bone-resorbing cells (osteoclasts) and bone-forming cells (osteoblasts) and hijack signals coming from the bone matrix.<sup>(1)</sup> Specifically, metastatic breast cancer cells enhance bone resorption and inhibit bone formation, and bone-derived growth factors released from resorbed bone stimulate skeletal tumor outgrowth.<sup>(1)</sup> The realization that breast cancer cells in the bone marrow promote skeletal destruction has led to

the use of therapies that inhibit the activity of bone-resorbing osteoclasts (bisphosphonates, denosumab).<sup>(2)</sup> However, these treatments are only palliative. They do not provide a life-prolonging benefit to patients, and a significant proportion of these patients with advanced breast cancer still experience bone complications.<sup>(2)</sup> Thus, cellular and molecular mechanisms implicated in the early dissemination of breast cancer cells in the bone marrow need to be better understood in order to improve current treatment modalities.

The blood of many patients with advanced breast carcinomas contains circulating tumor cells, at least a subset of which may extravasate and disseminate in the bone marrow.<sup>(3)</sup> These tumor cells disseminating in the bone marrow, in all probability,

Received in original form July 31, 2013; revised form February 13, 2014; accepted February 25, 2014. Accepted manuscript online March 11, 2014.

Address correspondence to: Dr Philippe Clézardin, INSERM, UMR1033, Faculté de Médecine Lyon-Est (domaine Laennec), Rue Guillaume Paradin, 69372 Lyon cedex 08, France. E-mail: philippe.clezardin@inserm.fr

Additional Supporting Information may be found in the online version of this article.

Journal of Bone and Mineral Research, Vol. 29, No. 8, August 2014, pp 1886–1899

DOI: 10.1002/jbmr.2215

© 2014 American Society for Bone and Mineral Research

represent the earliest sign of development of metastatic disease in patients. Indeed, their detection in the bone marrow correlates with a poor clinical outcome in breast carcinomas.<sup>(4)</sup> Additionally, a current hypothesis gaining ground is that disseminated tumor cells in the bone marrow (and circulating tumor cells in the blood) display a full or partial epithelial-to-mesenchymal transition (EMT), leading to mesenchymal traits such as loss of E-cadherin-mediated cell-cell adhesion, induction of invasiveness, and anchorage-independent growth.<sup>(3,5,6)</sup> EMT can also induce circulating and disseminating breast cancer cells to enter into a stem cell-like state, as exemplified by the expression of stem cell markers (such as CD44<sup>high</sup>/CD24<sup>low</sup>).<sup>(3,5,6)</sup> Interestingly, Twist1 has been reported as a link between EMT and stemness in breast carcinomas.<sup>(7)</sup> It is expressed in disseminated breast cancer cells that persist in the bone marrow after chemotherapy.<sup>(8)</sup> Yet its involvement in breast cancer bone metastasis formation is unknown.

Twist1 is a basic helix-loop-helix transcription factor initially identified as a major regulator of cell movement and tissue reorganization during early embryogenesis.<sup>(7)</sup> However, *TWIST1* is aberrantly reactivated in human cancers.<sup>(7)</sup> In clinical studies, *TWIST1* expression in primary breast tumors has been associated with disease aggressiveness and poor survival.<sup>(9)</sup> Indeed, *TWIST1* mediates escape to the oncogenic-induced failsafe program by preventing oncogene-induced senescence and apoptosis, which provides tumor cells with a growth advantage.<sup>(10)</sup> In mouse and human breast tumor xenograft models, *TWIST1* also promotes tumor cell invasion through activation of microRNA 10b (miR-10b), facilitating the intravasation of breast cancer cells in the systemic circulation and their dissemination to the lungs.<sup>(11–13)</sup> Additionally, the prometastatic effects of *TWIST1* are dependent on the activation of a CD44-lysyl oxidase (LOX) pathway that stimulates *TWIST1* transcription in breast cancer cells.<sup>(14)</sup> Thus, a number of experimental findings have been gathered demonstrating that *TWIST1* expression in breast cancer is associated with tumorigenesis and lung metastasis.

In the present study, we sought to explore the function(s) of *TWIST1* in experimental human breast cancer bone metastasis.

## Materials and Methods

### Cell lines, cell culture and transfection

The human B02 breast cancer cell line is a subpopulation of the MDA-MB-231 cell line that was selected for the high efficiency with which it metastasizes to bone in animals.<sup>(15)</sup> This cell line was authenticated using short tandem repeat analysis. The human MCF-7 and mouse 4T1 breast cancer cell lines were obtained from the American Type Culture Collection (ATCC, Manassas, VA, USA). The human mammary epithelial cell (HMEC) lines expressing the control vector pBABE-PURO or pBABE-PURO/*TWIST1* and characteristics of Tet-off-expressing B02 cells were previously described.<sup>(11,16)</sup> The cDNA encoding the entire human *TWIST1* was amplified by PCR and inserted into the pCi-Neo plasmid (Promega, Charbonnieres, France) to generate the pCi-Neo-Twist1. The bidirectional vector pBiL/*TWIST1* was constructed by inserting the Twist1 encoding sequence digested by NheI/NotI from the pCi-neo into the pBiL plasmid (Clontech). Tet-off-expressing B02 cells were cotransfected with pBiL/Twist1 together with a vector conferring puromycin resistance. Selection of the clones was obtained after growing the cells for 2 weeks in the presence of puromycin (2 µg/mL). Luciferase induction upon doxycycline (dox) withdrawal was used to select

inducible clones among stable transfectants. Two *TWIST1*-inducible transfectants (B02-Twist#112 and B02-Twist#135) and one negative control-inducible transfectant (B02-GFP/βGAL) encoding for β-galactosidase (βGAL) and luciferase were used in the present study. Inducible transfectants were routinely cultured in DMEM medium (Invitrogen, France) supplemented with 10% fetal bovine serum and 1% penicillin/streptomycin (Invitrogen) at 37°C in a 5% CO<sub>2</sub> incubator.

For the silencing of miR-10b in B02-Twist#135 and 4T1 cells, an antagomiR-10b and a negative control antagomiR were purchased from Applied Biosystems. Both cell lines were transfected with 50 nM of antagomiR-10b or negative control antagomiR using the HiPerFect transfection reagent (Qiagen, Courtabeuf, France). These antagomiRs were incubated with 1 × 10<sup>6</sup> cells for 30 minutes at 37°C in a 5% CO<sub>2</sub> incubator. Transfected cells were then grown in culture for 72 hours before tumor cell inoculation to animals. The efficiency of oligonucleotide delivery into these tumor cells was assessed using cell transfection with Alexa-fluor488-conjugated oligonucleotides followed by flow cytometry analysis of fluorescently-labeled transfected cells.

### Immunofluorescence

Dox-treated and untreated B02 transfectants were fixed in culture wells with 2% paraformaldehyde (Sigma) in PBS for 10 minutes and permeabilized with 0.2% (vol/vol) saponin in PBS for 10 minutes. The samples were washed with 10 mM glycine in PBS prior to blockage of aspecific sites with 10% (vol/vol) goat serum. Immunodetection was performed using a mouse monoclonal antibody against *TWIST1* (Twist2C1a; Abcam; dilution 1/100) or a rabbit polyclonal antibody against YB-1 (Abcam; dilution 1/1,000). Following overnight incubation at 4°C, cells were incubated for 1 hour with a secondary antibody (Alexa 488-conjugated goat anti-mouse for *TWIST1* and Alexa 488-conjugated goat anti-rabbit for YB-1) at a dilution of 1/1000 (Rockland, Tebu-bio). Nuclei were labeled for 10 minutes at room temperature with 4,6-diamidino-2-phenylindole (DAPI) at a concentration of 1 mg/mL in PBS. The distribution of F-actin was visualized after incubation of permeabilized cells for 50 minutes at room temperature with phalloidin (1/40 dilution; Molecular Probes), according to the manufacturer's instructions. Cells were observed using a LMS510 laser scanning confocal microscope (Zeiss, Le Pecq, France) with a 63× (numerical aperture 1.4) Plan Neo Fluor objective. To prevent contamination between fluorochromes, each channel was imaged sequentially, using the multi-track recording module, before merging.

### Western blotting

Total protein cell extracts were lysed in radioimmunoprecipitation assay (RIPA) buffer (Sigma) containing a protease cocktail inhibitor (Roche). Nuclear and cytoplasmic proteins were extracted from 4 × 10<sup>6</sup> cells using the NE-PER nuclear and cytoplasmic extraction kit (Thermo Scientific), according to the manufacturer's instructions. Protein cell extracts were electrophoresed on a 4% to 12% gradient SDS-polyacrylamide gel (Life Technologies), then transferred onto nitrocellulose membranes (Millipore, Billerica, MA, USA) and proteins were probed with a primary antibody against *TWIST1* (twist2C1a, 1/200 dilution; Abcam), YB1 (rabbit polyclonal antibody, 1/2000 dilution; Abcam), E-cadherin (goat polyclonal antibody, 1/2000 dilution; R&D Systems), vimentin (rabbit polyclonal antibody, 1/1000 dilution; BioVision), β-tubulin (CI B-512, 1/5000 dilution;

Sigma) or H4 histone (mabF-9, 1/1000; Santa Cruz Biotechnologies, Santa Cruz, CA, USA), according to the manufacturers' instructions. After incubation with primary antibodies, membranes were incubated with horseradish peroxide (HRP)-conjugated donkey anti-rabbit and anti-mouse secondary antibodies (Amersham; 1/2000 dilution), and immunostaining was performed with enhanced chemiluminescence (ECL) detection system (Perkin Elmer).

#### Real-time RT-PCR

Total RNA from human breast tumor cells was extracted using the Nucleospin RNA kit based on RNA adsorption on silica membrane further treated by rDNase (Macherey Nagel, Duren). cDNA was produced from 1 µg total RNA using the iScript cDNA Synthesis Kit (Bio-Rad, Hercules, CA, USA). Real-time quantitative PCR reactions were performed using a SYBR Green qPCR kit (Qiagen, Courtabeuf, France) on a Light-Cycler (Roche Diagnostics, Mannheim, Germany). Relative gene expression levels were normalized according to the threshold cycle ( $C_t$ ) value of the gene encoding the ribosomal protein L32 and results were expressed as fold differences equal to  $2^{-\Delta\Delta C_t}$ . In some experiments, *TWIST1* levels in B02 clones were expressed as copy number/µg RNA by absolute quantification, using a standard curve set up from  $2 \times 10^{11}$  to  $2 \times 10^2$  copies. PCR reactions were performed with the following primers: *TWIST1* forward 5'-GCAGGACGTGCCAGCTC-3', *TWIST1* reverse 5'-CTGGCTTCCCT-CGCTGTT-3'; *VEGF* forward, 5'-AGGAGGAGGGCAGAACATCAGAC-3', *VEGF* reverse 5'-TCTATCTTCTTGGTCTGCATT-3'; *DKK1* forward 5'-TAGCACCTGGATGGGTATT-3', *DKK1* reverse 5'-ATCCGTAGG-CACAGTCTGAT-3'; *YB-1* forward 5'-GGAGATGAGACCCAAGGTCA-3', *YB-1* reverse 5'-GGTAAGCGGGCATTTACTCA-3'; *LOX* forward 5'-GGATACGGCATGGCTACTTC-3', *LOX* reverse 5'-TTGGTCGGCT-GGCTAAGAAAT-3'; *LOXL2* forward 5'-CGGAGGATGTCGGTGTGGT-3', *LOXL2* reverse 5'-TGGCAGTCGATGTCGGCAT-3'; *CDH2* forward 5'-CCATCACTGGCTTAATGGT-3', *CDH2* reverse 5'-ACCCA-CAATCCTGTTCCACAT-3'; *RUNX2* forward 5'-GGAGTGGACGAGG-CAAGA-3', *RUNX2* reverse 5'-AGCTCTGTCTGTGCTCTGG-3'; *ZEB1* forward 5'-AGCAGTGAAAGAGAAGGAATGC-3', *ZEB1* reverse 5'-GGCCTCTTCAGGTGCTCAG-3'; *ZEB2* forward 5'-CAAGAGGCG-CAAACAAGC-3', *ZEB2* reverse 5'-GGTTGGCAATACCGTCATCC-3'; *SNAI1* forward 5'-TCGGAAGCCTAACTACAGCGA-3'; *SNAI1* reverse 5'-AGATGAGCATTGGCAGCGAG-3'; *SNAI2* forward 5'-AAGCATT-CAACGCCTCCAAA-3', *SNAI2* reverse 5'-GGATCTGGTTGTTGAT-GACA-3'; and *RPL32* forward 5'-CAAGGAGCTGGAAGTGCTGC-3', *RPL32* reverse 5'-CAGCTCTTCCACGATGGCT-3'.

TaqMan microRNA assays (Applied Biosystems, Life Technologies) were used to quantify miR-10b and RNU48 levels after extraction by cell homogenization in TRIzol reagent (Gibco). Ten (10) ng of total RNA were reverse-transcribed using the MultiScribe reverse transcriptase and 50 nM stem-loop RT primers specific for miR-10b and the endogenous control RNU48. Mature miRNAs were amplified using the TaqMan 2× universal PCR Master Mix and miR-10b levels were expressed as fold differences equal to  $2^{-\Delta\Delta C_t}$ .

#### Cell enumeration assay

Cell growth curves were done after seeding the cells ( $1 \times 10^4$  per well) into 12-well plates and cultured them up to 96 hours. Cells were harvested at various time points following trypsinization and single-cell suspensions were then counted by the True Volumetric Absolute Counting technique of flow cytometry (Partec Instruments).

#### Cell apoptosis assay

Cells in culture were serum-starved for 24 hours using DMEM medium supplemented with 0.1% (wt/vol) BSA then treated or not treated with camptothecin (a proapoptotic drug) for 6 hours. These cultured cells were then detached with Accutase, washed twice with cold PBS and resuspended in Annexin V binding buffer at a concentration of  $1 \times 10^6$  cells/mL, according to the manufacturer's instructions (BD Pharmingen). Cells in suspension were stained with phycoerythrin (PE)-AnnexinV and the vital dye 7-amino-actinomycin (7-AAD). Early apoptotic cells will exclude 7-AAD, whereas late-stage apoptotic cells will stain positively, due to the passage of the dye into the nucleus where it binds to DNA. Cell apoptosis was measured by flow cytometry.

#### Cell invasion assay

Experiments were conducted in 24-well cell culture plates with 8-µm-diameter pore-size inserts, coated with 100-µL basement membrane Matrigel (0.3 mg/mL), as described.<sup>(17)</sup> Untreated and dox-treated B02 transfectants ( $1.6 \times 10^5$  cells/mL) and control- and *TWIST1*-expressing HMEC cells ( $5 \times 10^5$  cells/mL) were resuspended in culture medium containing 0.1% (wt/vol) bovine serum albumin and 300 µL of this cell suspension were loaded into each insert (upper chamber). The chemoattractant (10% v/v fetal calf serum) was placed in the lower chamber (750 µL/well). After a 24-hour incubation at 37°C in a 5% CO<sub>2</sub> incubator, inserts were collected, the non-invading cells were removed, and the invading cells on the under surface of the inserts were fixed and stained with crystal violet. Cells were then counted under a microscope.

#### Animals

Four-week-old female Balb/c immunocompromised mice were purchased from Charles River Laboratories (St. Germain sur l'Arbresle, France). All procedures involving animals, including their housing and care, the method by which they were culled, and experimental protocols were conducted in accordance with a code of practice established by the local ethical committee of the University of Lyon.

#### Animal studies

Orthotopic tumor xenograft experiments were conducted, as described.<sup>(17)</sup> Four-week-old female *nude* mice treated with dox or left untreated were injected in the fat pad of the fourth mammary gland with dox-treated or untreated transfectants ( $1 \times 10^6$  cells in 50 µL PBS), respectively. Tumor size was calculated by external measurement of the width ( $m_1$ ) and length ( $m_2$ ) of tumor xenografts using a Vernier caliper. Tumor volume (TV) was calculated using the equation  $TV = (m_1^2 \times m_2)/2$ . At the end of the protocols, mice were euthanized and tumors were collected then prepared for immunohistochemistry.

Bone metastasis experiments were conducted in female Balb/c *nude* mice, as described.<sup>(15-18)</sup> Dox-treated or untreated transfectants ( $5 \times 10^5$  cells in 100 µL PBS) were injected into the tail artery of anesthetized *nude* mice treated with dox or left untreated, respectively. Animals received or did not receive dox in the water supply (containing sucrose) for the duration of the experiments. Radiographs of anesthetized animals were taken weekly with the use of MIN-R2000 films (Kodak, Rochester, NY, USA) in an MX-20 cabinet X-ray system (Faxitron X-ray Corporation, Wheeling, IL, USA). Osteolytic lesions were identified on radiographs as radiolucent lesions in the bone. The area

of osteolytic lesions was measured using a computerized image analysis system, and the extent of bone destruction per leg was expressed in square millimeters. For measurement of skeletal tumor burden, bioluminescence imaging of animals was performed weekly using the Nightowl imaging system (Berthold, Germany), as described.<sup>(15–18)</sup> On day 32 after tumor cell inoculation, anesthetized mice were euthanized by cervical dislocation after radiography and bioluminescence imaging.

For ex-vivo bone marrow micrometastasis experiments, dox-treated or untreated B02 transfectants ( $5 \times 10^5$  cells in 100  $\mu\text{L}$  PBS) were injected into the tail artery of animals treated with dox or left untreated, respectively. Alternatively, animals were inoculated with B02-Twist#135 or 4T1 cells transfected with antagomir-10b ( $5 \times 10^5$  cells in 100  $\mu\text{L}$  PBS). Animals were then culled on day 7 after tumor cell inoculation. Hind limbs were collected and tibias and femurs were minced then soaked in an enzyme cocktail containing 300 U/mL type-I collagenase and 100 U/mL hyaluronidase (StemCell Technologies) in DMEM medium for 2 hours at 37°C. Lungs were minced and an enzyme solution containing 0.25 mg/mL type-I collagenase (Sigma) was added for 1 hour at 37°C. After incubation, cell suspensions from bone marrow and lungs were seeded in six-well plates and cultured in complete medium. After 1 day of culture, B02-Twist#135 and 4T1 cells were placed under antibiotic selection for 2 weeks (puromycin and 6-thioguanine, respectively), allowing the selective growth of antibiotic-resistant tumor cells. Colonies of tumor cells were then fixed, stained with crystal violet, and counted.

#### Bone histology, histomorphometry, and immunohistochemistry

Bone histology and histomorphometric analysis of bone tissue sections were performed as described.<sup>(15–18)</sup> Histomorphometric measurements (bone volume [BV]/tissue volume [TV] and tumor volume [TuV]/soft tissue volume [STV] ratios) were performed in a standard zone of the tibial metaphysis, situated at 0.5 mm from the growth plate, including cortical and trabecular bone. The BV/TV ratio represents the percentage of bone tissue. The TuV/STV ratio represents the percentage of tumor tissue. The *in situ* detection of osteoclasts was performed on tartrate-resistant acid phosphatase (TRAP)-stained longitudinal paraffin-embedded medial sections of tibial metaphysis with the use of a commercial kit (Sigma). Osteoclast resorption surface was calculated as the ratio of TRAP-positive trabecular bone surface to the total trabecular bone surface at the tumor–bone interface.

For immunohistochemistry, tumor sections were incubated with a mouse anti-human Ki67 monoclonal antibody (DakoCytomation) or a rabbit polyclonal anti-CD31 antibody (AnaSpec) that specifically recognize proliferative cells and blood vessels, respectively. The mitotic index and tumor microvessel density were quantified, as described.<sup>(18)</sup>

#### Osteoclastogenesis assay

Experiments were conducted as described,<sup>(16–18)</sup> with minor modifications. Briefly, murine bone marrow cells were cultured in α-MEM medium containing 10% (vol/vol) fetal calf serum supplemented with macrophage colony-stimulating factor (M-CSF) (20 ng/mL) and RANK-L (30 ng/mL), in the presence of conditioned medium from transfectants (20  $\mu\text{g}/\text{mL}$ ). A low concentration of RANKL was chosen in this study in order to maximize potential differences between conditioned media

from B02-Twist#135 cells expressing or not expressing TWIST1. After 7 days, mature osteoclasts were enumerated under a microscope on the basis of the number of nuclei (more than three nuclei) and TRAP activity. Results were expressed as the number of osteoclasts per well. The expression of genes involved in osteoclast differentiation and activity was analyzed by RT-qPCR, as described.<sup>(19)</sup>

#### Cytokine array

A commercial antibody-based protein microarray designed to detect 23 proteins including growth factors, cytokines, and chemokines (RayBio Human Cytokines Array 1, RayBiotech) was used. Array membranes were incubated for 2 hours with the conditioned medium from cultured transfected cells (150  $\mu\text{g}/\text{mL}$ ). After washing, membranes were incubated with a cocktail of 23 biotinylated antibodies, and the remaining experimental procedure was carried out following the manufacturer's instructions.

#### Flow-cytofluorometric analysis

Untreated and dox-treated B02-Twist#135 cells ( $1 \times 10^6$  cells in 500  $\mu\text{L}$  PBS supplemented with 1% BSA) were stained with a phycoerythrin-conjugated human anti-CD24 or a fluorescein-isothiocyanate-conjugated human anti-CD44 monoclonal antibody (BD Biosciences). Stained cells were then immediately analyzed by flow cytometry (Canto II; Becton Dickinson).

#### Statistical analysis

All data were analyzed using StatView software (version5.0; SAS Institute Inc, Cary, NC). Pairwise comparisons were carried out by performing a nonparametric Mann-Whitney *U* test. *p* values less than 0.05 were considered statistically significant. All statistical tests were two-sided.

## Results

#### Structural and functional characterization of TWIST1-expressing B02 transfectants

To investigate the role of TWIST1 in bone metastasis, we chose the human osteotropic MDA-MB-231/B02 breast cancer cell line (named B02 for brevity). The B02 breast cancer cell line is a subpopulation of the MDA-MB-231 cancer line that was selected for the high efficiency with which it metastasizes to bone in animals.<sup>(15)</sup> Like many other basal breast cancer cell lines, MDA-MB-231 (Supporting Fig. S1) and B02 cells did not express Tw1. B02 cells were stably transfected with a Tet-inducible bidirectional vector encoding for TWIST1 and luciferase, whose expression was specifically repressed in the presence of dox. A negative control cell line was obtained by introducing a pBI-L bidirectional Tet-inducible vector encoding for β-galactosidase and luciferase (B02-Ctrl).<sup>(16)</sup> Two TWIST1-inducible clones (B02-Twist#112 and B02-Twist#135) were selected on the basis of a specific TWIST1 expression upon dox withdrawal. TWIST1 levels in B02-Twist#112 and #135 cells were moderate and high, respectively (Supporting Fig. S2). B02-Twist#135 cells expressed  $2 \pm 0.014 \times 10^8$  copies/ $\mu\text{g}$  RNA of TWIST1, as assessed by RT-qPCR analysis, whereas B02-Twist#112 cells had 3.5 fewer copies. Analysis of B02-Twist#135 cells by confocal microscopy showed that TWIST1 was specifically localized in the nucleus. Dox treatment of B02-Twist#135 cells led to an almost complete

repression of *TWIST1*, as judged by both confocal microscopy and immunoblotting (Fig. 1A, B).

Although B02 cells did not express *TWIST1*, many other genes encoding for EMT-inducing transcription factors, including *SNAI1* (Snail), *SNAI2* (Slug), *ZEB1* and *ZEB2*, were highly expressed in these mesenchymal cells, compared with that observed for MCF-7 breast cancer cells, which have an epithelial phenotype (Supporting Table 1). Additionally, B02 cells lost the expression of the epithelial marker E-cadherin, whereas they expressed the mesenchymal marker vimentin (Fig. 1C). The expression of these transcription factors and vimentin, and the loss of E-cadherin

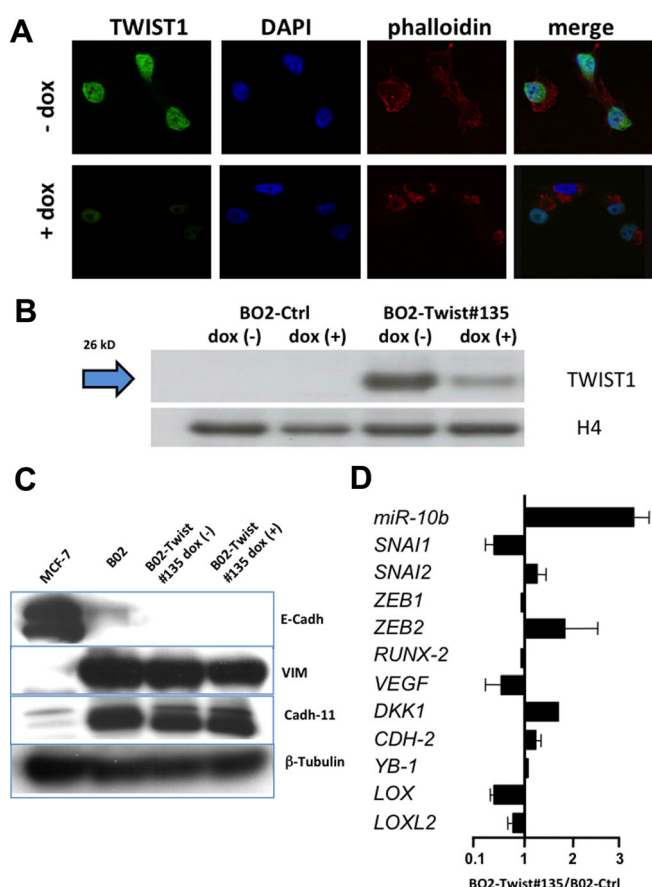


**Fig. 1.** Ectopic expression of *TWIST1* in mesenchymal human B02 breast cancer cells upregulates microRNA-10b. (A) Representative images by confocal microscopy showing the expression of *TWIST1* (green) in untreated [dox (-)] and doxycycline-treated [dox (+)] B02-Twist#135 cells. Dox almost completely repressed the nuclear expression of *TWIST1* in B02#135 cells, compared with that observed with untreated cells. DAPI (blue) and phalloidin (red) were used as reporters for the nuclei and cytoskeleton, respectively. (B) Mock-transfected B02 cells (MDA-B02-Ctrl) and B02-Twist#135 cells, treated or not treated with dox, were subjected to Western immunoblotting with antibodies against *TWIST1* or H4 histone (control for equal loading). B02-Ctrl cells do not express *TWIST1*. Dox repressed *TWIST1* expression in B02-Twist#135 cells. (C) Immunoblotting of E-cadherin (E-Cadh), vimentin (VIM), cadherin-11 (Cadh-11), and β-tubulin in MCF-7 and parental B02 breast cancer cells, and untreated and dox-treated B02-Twist#135 cells. (D) Effects of *TWIST1* on target gene expression in B02 cells. Relative transcript levels are represented as the ratios between B02-Twist#135 and B02-Ctrl real-time PCR values.

likely explained the spindle-like, fibroblastic morphology of B02 cells (not shown). This morphological change is one of the hallmarks of an EMT. Ectopic *TWIST1* expression in B02-Twist#135 cells did not, however, further modify the morphological appearance of these cells (not shown) and, at the molecular level, it did not alter cadherin-11 expression (Fig. 1C). Cadherin-11 is an osteoblast cadherin whose expression correlates with the osteotropic properties of B02 cells.<sup>(20)</sup> Conversely, *TWIST1* regulated the expression of zinc-finger transcription factors. An inverse transcriptional link between *TWIST1* and *SNAI1* in MCF10A mammary epithelial cells has been suggested.<sup>(21)</sup> Additionally, ectopic *TWIST1* expression in human HMLE mammary epithelial cells induces *SNAI2* transcription.<sup>(22)</sup> In agreement with these findings,<sup>(21,22)</sup> we observed here that *TWIST1* had a slight impact on expression of these two transcription factors, regulating *SNAI1* and *SNAI2* in a negative and positive manner, respectively (Fig. 1D). It also increased *ZEB2* transcription, but not *ZEB1* transcription (Fig. 1D). Compared with parental B02 cells, *TWIST1* ectopic expression did not affect or merely modestly modulated expression of other target genes,<sup>(23–26)</sup> such as transcription factor *YB-1* (a transcription factor associated with breast cancer cell proliferation), Dickkopf-1 (*DKK-1*; an inhibitor of canonical Wnt signaling), vascular endothelial growth factor (*VEGF*), *CDH-2* (N-cadherin), and *RUNX-2* (an osteoblastic transcription factor) (Fig. 1D). By contrast, it induced a 3.5-fold increase of miR-10b expression in B02#135 cells (Fig. 1D). *LOX*, but not *LOXL2* (*LOX-like 2*), was modestly repressed (Fig. 1D). In agreement with previous studies,<sup>(7)</sup> ectopic *TWIST1* expression also modestly but significantly increased stemness traits of B02 cells, which were already *CD44*<sup>high</sup>/*CD24*<sup>low</sup>, increasing the percentage of *CD44*-positive cells from 75% to 91.4% upon dox withdrawal (Supporting Fig. S3). All of the B02 cells were *CD24*<sup>low</sup>, irrespective of *TWIST1* expression (Supporting Fig. S3).

We next examined whether ectopic *TWIST1* expression affects B02 breast cancer cell functions in vitro. B02-Ctrl and B02-Twist#135 cells grew at a similar rate in the presence or absence of dox, indicating that *TWIST1* was not required for the proliferation of B02 breast cancer cells, when growing in vitro (Fig. 2A). These results were in line with the observation that *TWIST1* did not affect *YB-1* production, as determined by immunoblotting and confocal microscopy (Fig. 2B; data not shown). *TWIST1* did not affect tumor cell apoptosis either, whether B02-Twist#135 cells, when deprived of serum, were treated or not treated with camptothecin (a proapoptotic agent) (Supporting Fig. S4). By contrast, *TWIST1* ectopic expression in B02#135 cells substantially enhanced tumor cell invasion and promoted miR-10b expression, when compared with B02-Ctrl cells (Fig. 2C, D). Furthermore, both the increased cell invasiveness and enhanced miR-10b expression were abrogated in dox-treated B02-Twist#135 cells (Fig. 2C, D). Thus, *TWIST1* contributed to the invasive phenotype of B02 breast cancer cells in vitro. Similar results were obtained with immortalized HME mammary epithelial cells where ectopic *TWIST1* expression also promoted both cell invasiveness and miR-10b expression (Fig. 2E, F), indicating that the proinvasive effect of *TWIST1* was not restricted to B02-Twist#135 cells.

#### *TWIST1* ectopic expression enhances breast cancer bone metastasis formation

To determine whether *TWIST1* plays a causal role in bone metastasis, luciferase-expressing B02-Ctrl or B02-Twist#135 cells

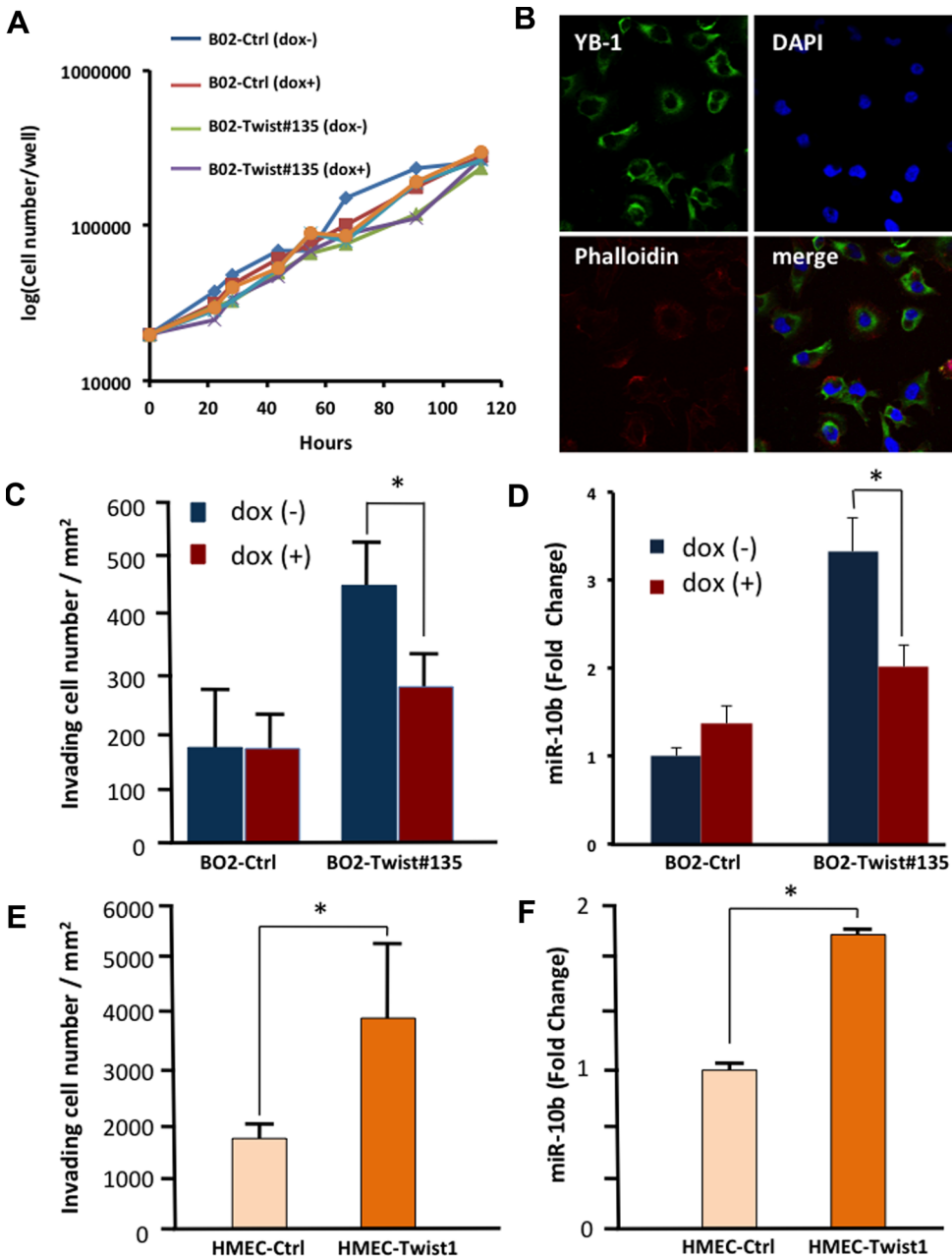


**Fig. 2.** *TWIST1* ectopic expression promotes invasion but is a dispensable transcription factor for the proliferation of human B02 breast cancer cells in vitro. (A) Proliferation rates of untreated and dox-treated mock-transfected (B02-Ctrl) and *TWIST1*-expressing B02 cells (B02-Twist#135). (B) Representative images by confocal microscopy showing the expression of YB-1 (green) in B02-Twist#135 cells. DAPI (blue) and phalloidin (red) were used as reporters for the nuclei and cytoskeleton, respectively. (C) Cell invasion assay. Untreated and dox-treated B02 clones (B02-Ctrl and B02-Twist#135) were loaded in inserts with a porous membrane coated with basement membrane Matrigel (upper chamber) and the chemoattractant (serum) was placed in wells of a companion plate (lower chamber). After a 24-hour incubation at 37°C, the non-invading cells were removed and the invading cells on the under surface of the inserts were fixed, stained, and counted under a microscope. \* $p < 0.05$ . (D) miR-10b expression in untreated and dox-treated B02-Ctrl and B02-Twist#135 cells. miR-10b expression level in untreated B02-Ctrl cells was set to 1. Data were then expressed as a fold-change of miR-10b expression compared with that observed in untreated B02-Ctrl cells. \* $p < 0.05$ . (E, F) Same as C and D, showing the effects of *TWIST1* on invasion and miR-10b production by immortalized human mammary epithelial cell (HMEC) lines expressing the control vector (HMEC-Ctrl) or *TWIST1* (HMEC-Twist1), respectively.

were injected into the tail artery of immunodeficient mice. Bioluminescence imaging of animals bearing B02-Twist#135 tumors showed tumor take in hind limbs as early as on day 7 after tumor cell inoculation, then skeletal tumor burden progressively increased over time (Fig. 3A). There was no

bioluminescence in organs other than bone, indicating that ectopic *TWIST1* expression did not modify the bone tropism of B02 breast cancer cells in vivo. However, tumor take in hind limbs of animals bearing B02-Twist#135 tumors occurred much earlier than that observed in animals bearing B02-Ctrl tumors

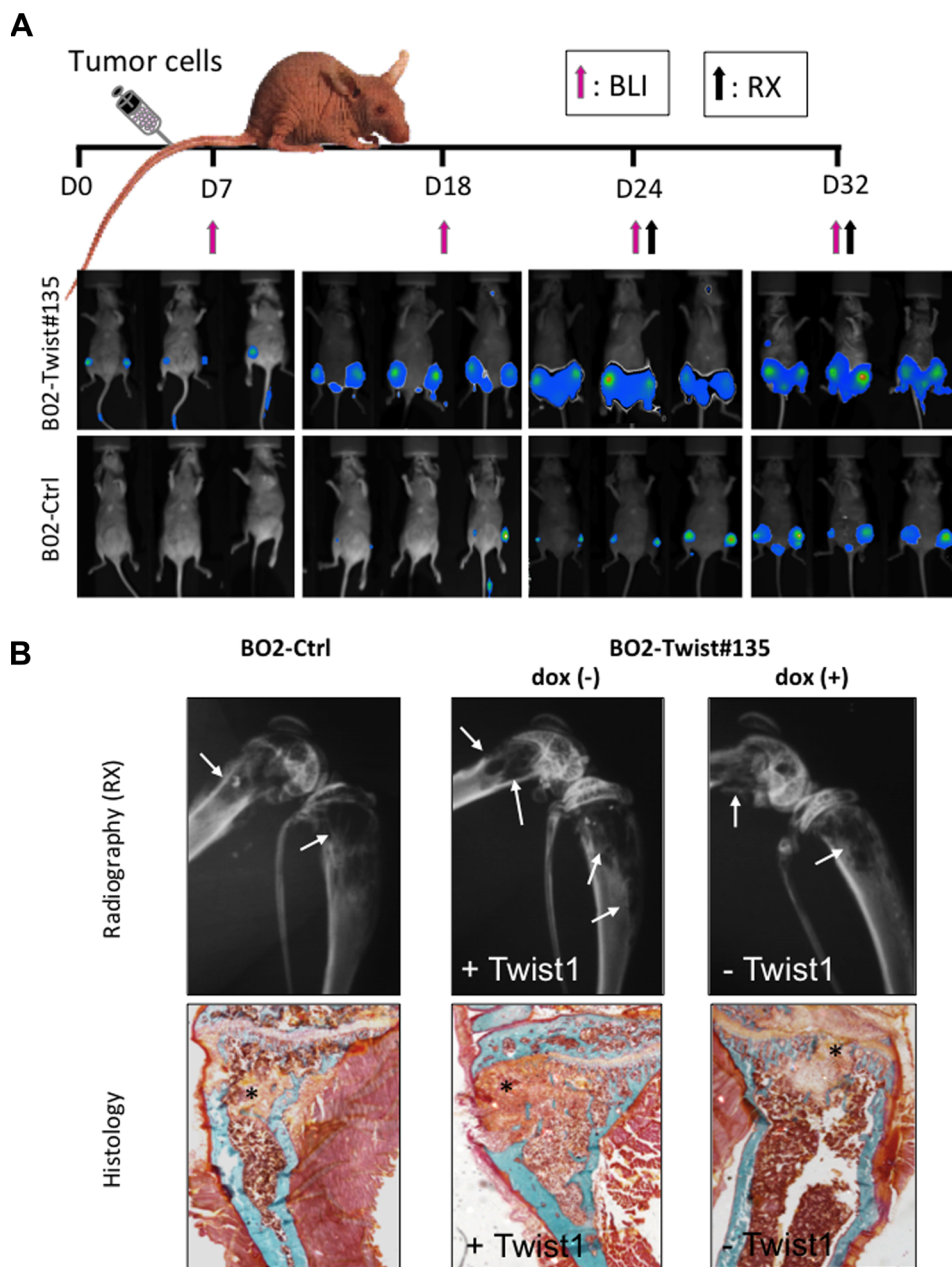


**Fig. 3.** *TWIST1* ectopic expression promotes breast cancer bone metastasis formation. (A) Upper panel: Summary of the experimental bone metastasis protocol. B02-Ctrl cells or B02-Twist#135 cells [treated or not treated with doxycycline (dox)] were inoculated into female Balb/c *nude* mice on day 0. Animals then received or did not receive dox in the water supply for the duration of the experiment. Animals were analyzed by bioluminescence imaging (BLI) and radiography (RX) at scheduled intervals. Bottom panels: For BLI, representative images of animals inoculated with B02-Twist#135 cells or B02-Ctrl cells were shown at different time intervals after tumor cell inoculation. These images best illustrate the effect of *TWIST1* on skeletal tumor burden. (B) Upper panels: Radiographic analysis of hind limbs from mice bearing B02-Ctrl or B02-Twist#135 tumors. *TWIST1* expression in B02#Twist-135 cells was turned off by dox [dox (+)]. Arrows indicate osteolytic lesions. Bottom panels: Goldner's trichrome staining of tissue sections of tibial metaphysis. Bone is stained green whereas bone marrow and tumor cells (asterisk) are stained red. All images were obtained from different mice on day 32 after tumor cell inoculation. The images shown are examples that best illustrate *TWIST1*'s effects on bone destruction and tumor burden.

(Fig. 3A). This observation suggested that the expression of *TWIST1* in B02 cells promoted tumor cell invasion in the bone marrow microenvironment.

Radiographic analysis on day 32 after tumor cell injection revealed that the extent of osteolytic lesions in hind limbs of

animals bearing B02-Twist#135 tumors was increased, being 50% larger than that of animals bearing B02-Ctrl tumors (Table 1, Fig. 3B). Compared with B02-Ctrl tumor-bearing mice, there was also a substantial increase in the extent of osteolytic lesions in animals bearing B02#Twist-112 tumors (Supporting Fig. S5).

**Table 1.** Effects of *TWIST1* Expression in B02 Breast Cancer Cells on Bone Metastasis Formation in Animals Treated or Not Treated With Doxycycline

Cell line	Radiography		Histomorphometry			TRAP staining		
	mm <sup>2</sup> /mouse	p	BV/TV (%)	p	TuV/STV (%)	p	OC.S/BS (%)	p
B02-Ctrl	4.1 ± 0.3 (n = 11)	—	21.4 ± 8.1 (n = 11)	—	41.7 ± 12.9 (n = 11)	—	45.9 ± 22.8 (n = 5)	—
B02-Twist#135	8.2 ± 0.5 (n = 10)	0.01	7.7 ± 4.2 (n = 10)	0.001	72.4 ± 16.6 (n = 10)	0.0007	33.5 ± 6.1 (n = 5)	NS
B02-Twist#135 + doxycycline	3.2 ± 0.4 (n = 5)	0.02	20.4 ± 2 (n = 5)	0.533	25.8 ± 16.2 (n = 5)	0.027	36.9 ± 11.4 (n = 5)	NS

Values are mean ± SD. Values of p (two sided) are for pairwise comparison with the control group using the Mann-Whitney U test. All measurements were performed 32 days after tumor cell injection.

TRAP = tartrate-resistant acid phosphatase; BV/TV = bone volume-to-tissue volume ratio; TuV/STV = tumor volume-to-total soft tissue volume ratio; OC.S/BS = active osteoclast-resorption surface per trabecular bone surface; B02-Ctrl = control B02 breast cancer cells expressing the doxycycline-inducible vector encoding for β-galactosidase (Tet-Off system); — = not applicable (referent); B02-Twist#135 = B02 breast cancer expressing the doxycycline-inducible vector encoding for *TWIST1*; NS = not significant.

Additionally, on day 24 after tumor cell injection, osteolytic lesions in hind limbs of animals bearing B02#Twist-135 tumors were statistically significantly larger than those of animals bearing B02#Twist-112 tumors, indicating that there was a correlation between *TWIST1* expression levels in B02 cells and the extent of bone destruction in vivo (Supporting Fig. S5). This difference was accompanied with a sharp reduction of the BV/TV ratio (indicating a higher bone destruction) and a twofold increase in the TuV/STV ratio (a measure of the skeletal tumor burden) (Table 1, Fig. 3B). Importantly, the *TWIST1*-related stimulatory effects on bone destruction and skeletal tumor burden were abolished in dox-fed animals, indicating that *TWIST1* expression in tumor cells was responsible for enhanced bone metastasis formation in vivo (Table 1, Fig. 3B).

Compared with dox-fed animals, the overall TRAP staining of bone tissue sections of metastatic legs from untreated mice bearing B02-Twist#135 tumors was increased (Fig. 4A). However, ratios of TRAP staining surfaces over bone surfaces at the tumor-bone interface were similar, irrespective of *TWIST1* expression (Table 1). This showed that bone destruction in metastatic legs from animals bearing B02-Twist#135 tumors increased as a function of the skeletal tumor burden; the higher the tumor burden, the higher the bone destruction (Table 1). To further address this question, a human cytokine antibody array was used to measure cytokines in the conditioned medium from B02#Twist-135 cells, treated or not treated with dox. Several cytokines and interleukins known to stimulate osteoclast differentiation (MCP-1, GM-CSF, IL-6, IL-8) were produced by these cells (Fig. 4B). Cytokine profiles produced by B02#Twist-135 cells were, however, similar, irrespective of *TWIST1* expression (Fig. 4B). Additionally, to directly test whether ectopic *TWIST1* expression in B02 cells could influence osteoclast differentiation, we treated primary mouse bone marrow cell cultures with RANKL and M-CSF, which are two hematopoietic factors both necessary to induce osteoclastogenesis, together with the conditioned medium of untreated or dox-treated B02#Twist-135 cells. Consistent with in vivo data (Fig. 4A), the conditioned media of B02-Twist#135 cells treated or not treated with dox stimulated the formation of TRAP-positive multinucleated osteoclasts to a similar extent (Fig. 4C). Therefore, ectopic *TWIST1* expression did not enhance the intrinsic ability of B02 cells to stimulate osteoclast differentiation. Compared with the conditioned medium of dox-treated B02-Twist#135 cells, the conditioned medium of untreated B02-Twist#135 cells did, however, stimulate osteoclast activity as judged by a twofold increase in Ctsk

expression (Fig. 4D), a gene encoding for cathepsin K, an osteoclast-derived cysteine protease enabling degradation of the collagenous matrix.<sup>(1)</sup> Conversely, the expression of other markers associated with osteoclast differentiation (eg, Trap, Calcr, Car2) and morphology (eg, Itgb3) was not affected (Fig. 4D). Additionally, *TWIST1* in B02 cells did not modulate osteoblast differentiation in vitro (data not shown). Hence, our observations pointed to a specific role of *TWIST1* in promoting skeletal tumor outgrowth and osteoclast activity.

#### *TWIST1* ectopic expression accelerates tumor establishment but has no effect on growth rates of breast tumors into the mammary gland

To determine whether *TWIST1* affects B02 cells to form primary tumors in vivo, B02#Twist-135 tumor cells were injected into the mammary fat pads of untreated or dox-fed female *nude* mice. *TWIST1* expression induced a rapid tumor take in untreated animals compared with dox-fed animals (Fig. 5A). Untreated B02#Twist-135 tumor cells formed tumors within 5 to 6 weeks of inoculation, whereas it took an additional 4 weeks for dox-treated B02#Twist-135 cells to grow as palpable tumors. However, once B02-Twist#135 tumors were established, those expressing *TWIST1* grew at the same rate as tumors where *TWIST1* was repressed (Fig. 5A). Immunostaining of B02-Twist#135 tumors for Ki67 (a measure of tumor cell proliferation) and CD31 (a measure of the microvessel density) showed, respectively, that the proliferative index and the vascularization of tumors were similar regardless of *TWIST1* expression (Fig. 5B). In the same vein, B02#Twist-112 cells, which produced moderate *TWIST1* levels (Supporting Fig. S2), only modestly accelerated tumor establishment in untreated animals, compared with that observed in dox-fed animals (Supporting Fig. S6). Additionally, once tumors were established, untreated and dox-treated B02#Twist-112 cells formed primary mammary tumors at similar rates (Supporting Fig. S6). Hence, *TWIST1* was not required for primary tumor growth formation. However, *TWIST1* expression levels correlated with the onset of tumor establishment into the mammary gland.

#### *TWIST1* promotes the engraftment of breast cancer cells in the bone marrow through a process dependent of miR-10b

Because *TWIST1* promoted breast tumor establishment into the mammary fat pad of animals, we hypothesized that this

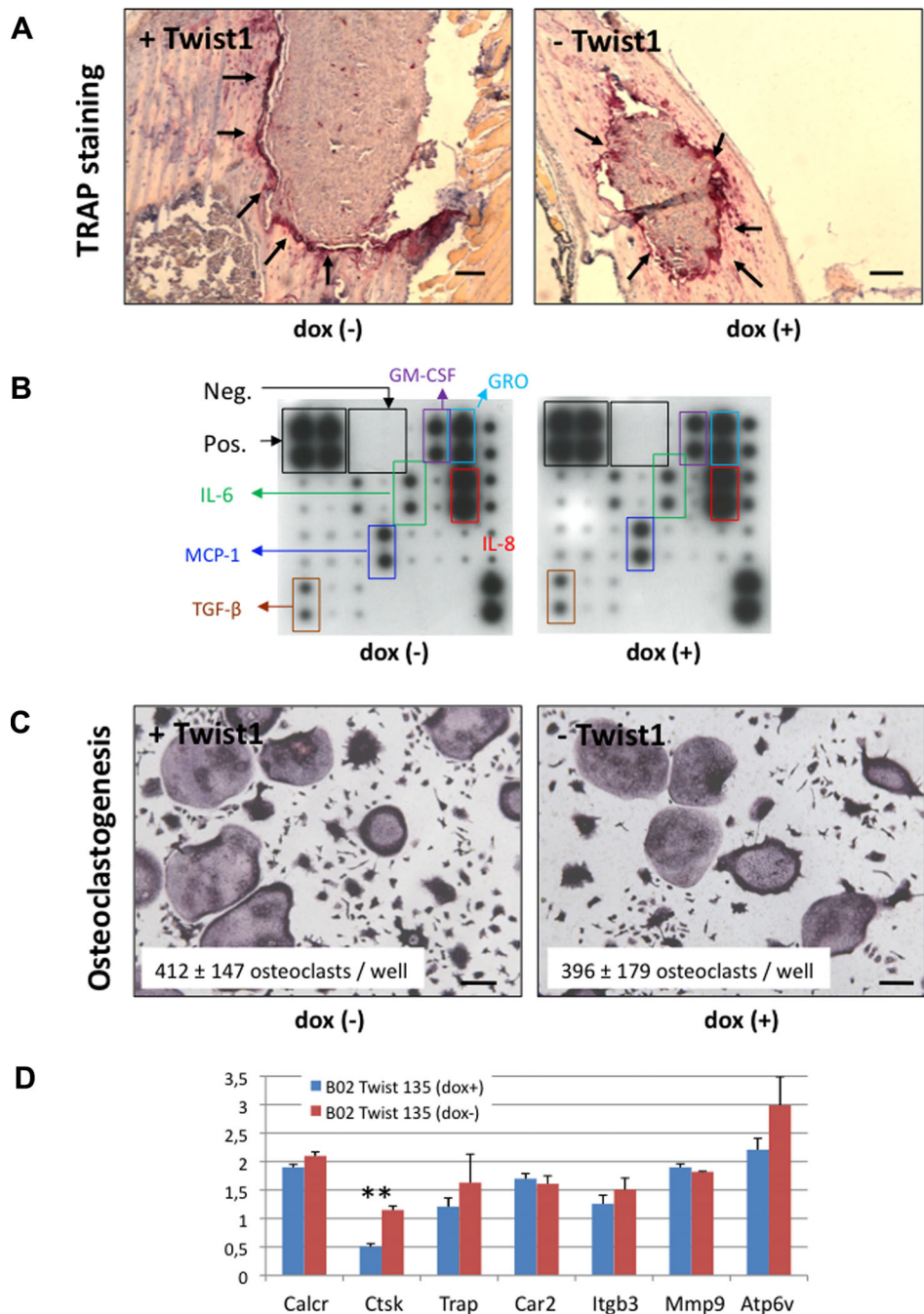


**Fig. 4.** TWIST1 ectopic expression in B02 breast cancer cells does not affect osteoclast differentiation, but it stimulates osteoclast activity. (A) TRAP-stained metastatic bone tissue sections from animals treated (+) or not treated (-) with doxycycline (dox). Osteoclasts are stained red. (B) Antibody-based protein microarray enabling detection of cytokines produced in the conditioned medium from B02-Twist#135 cells that were cultured in the presence or absence of dox. (C) In vitro osteoclast differentiation of murine bone marrow cells treated with M-CSF + RANKL in combination with the conditioned medium from untreated or dox-treated B02-Twist#135 cells. Mature osteoclasts were quantified as multinucleated (more than 3 nuclei), TRAP-positive cells. Representative images of mature osteoclasts are shown for each group. (D) RT-qPCR analysis of murine osteoclasts treated with the conditioned medium from untreated or dox-treated B02-Twist#135 cells. Data are representative of three separate experiments. \*\* $p < 0.005$ . Calcr = calcitonin receptor; Ctsk = cathepsin K; Trap = tartrate-resistant acid phosphatase; Car2 = anhydrase carbonic; Itgb3 = integrin beta-3; Mmp9 = matrix metalloprotease 9; Atp6v = V-ATPase.

transcription factor might also facilitate the engraftment of B02 cells in the bone marrow microenvironment. To address this question, dox-treated or untreated B02-Twist#135 cells were injected into the tail artery of animals treated with dox or left

untreated, respectively, and these animals were then culled on day 7 after tumor cell inoculation, at which time there was no evidence of metastases, as judged by radiography. The bone marrow was collected from the hind limbs of these animals and

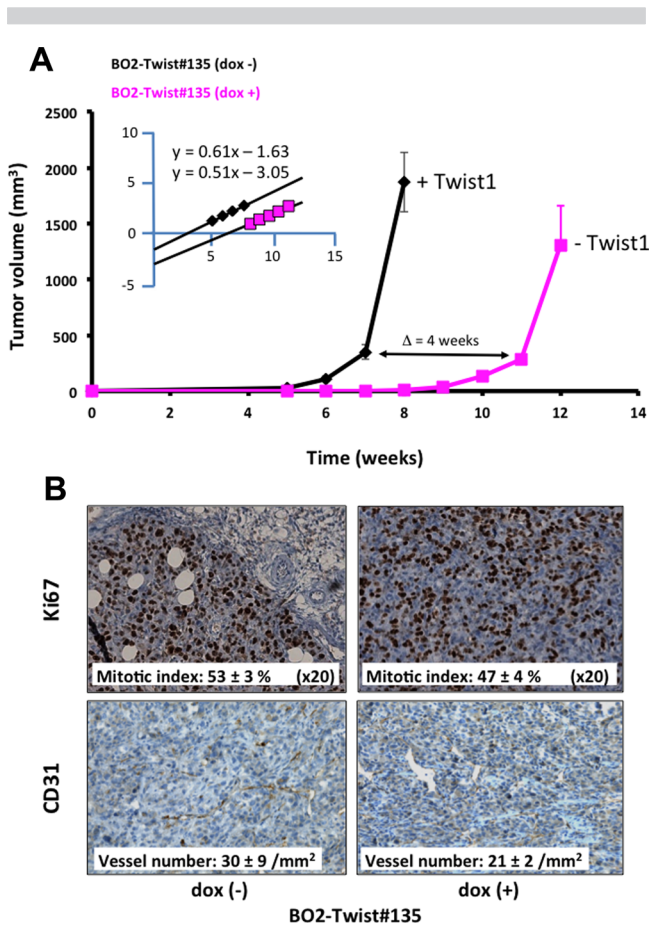


**Fig. 5.** *TWIST1* ectopic expression in B02 breast cancer cells accelerates tumor establishment in animals. (A) B02#Twist-135 tumor cells were injected orthotopically in female mice receiving or not receiving doxycycline (dox) in drinking supply. *TWIST1* expression in B02#Twist-135 cells was turned off by dox. Tumor volumes were measured with a Vernier caliper. Inset: Logarithmic conversion of the growth curves. (B) Ki67 and CD31 immunostaining of tissue sections of harvested B02-Twist#135 tumors from untreated and dox-treated animals at weeks 8 and 12, respectively, as a measurement of the proliferative index of tumor cells and number of tumor-associated blood vessels.

placed in culture under antibiotic selection, allowing the selective growth of antibiotic-resistant tumor cells. The incidence and number of colonies formed by B02 cells were then quantified. We recovered tumor cell colonies from 4 of 5 untreated animals injected with B02-Twist#135 cells (Fig. 6A). In sharp contrast, under the same experimental conditions, tumor cell colonies were recovered from the bone marrow of 1 of 5 dox-fed animals. Moreover, the average number of colonies recovered from the bone marrow of the 4 mice bearing B02-Twist#135 cells (89 colonies/well) was much higher than that recovered from the single mouse bearing dox-treated B02-Twist#135 cells (2 colonies/well) (Fig. 6A). This observation strongly suggested that *TWIST1* expression enhanced the presence of B02 cells in the bone marrow.

We next undertook to determine how *TWIST1* could promote engraftment of B02 breast cancer cells in the bone marrow. The observations that miR-10b was upregulated by *TWIST1* in B02-Twist#135 cells (Fig. 2D) and that miR-10b induces breast tumor

invasion *in vivo*<sup>(13)</sup> led us to ask whether miR-10b might mediate *TWIST1*-dependent engraftment of B02 cells in the bone marrow. We therefore silenced miR-10b in B02-Twist#135 cells using an antagomir. As assessed by RT-qPCR, miR-10b expression was suppressed by more than 70% in the presence of antagomir-10b (data not shown). Transfected cells silenced for miR-10b were then inoculated into animals. On day 7 after tumor cell inoculation, colonies were recovered from the bone marrow of only 2 of 5 mice, whereas tumor cell colonies were recovered from all of the 5 animals inoculated with control B02-Twist#135 cells (Fig. 6B). Additionally, the average number of colonies recovered from the bone marrow of the 2 mice bearing B02-Twist#135 cells silenced for miR-10b (26 colonies/well) was much smaller than that recovered from the 5 mice bearing control B02-Twist#135 cells (65 colonies/well) (Fig. 6B). Hence, miR-10b silencing in *TWIST1*-expressing B02 cells led to a substantial reduction of the incidence and number of tumor cell colonies in the bone marrow.

We wished to determine whether the ability of miR-10b to mediate engraftment of B02 cells in the bone marrow could be extended to another breast cancer cell line (4T1) that spontaneously metastasizes to the bone marrow and lungs in animals. *Twist1* directly regulates miR-10b expression in 4T1 cells.<sup>(13)</sup> Mouse 4T1 cells were therefore transfected with an antagomir-10b then inoculated into the tail artery of immunocompetent mice. At day 7 after tumor cell inoculation, the bone marrow and lung extracts of these animals were collected and cells derived from these tissues were placed in culture under 6-thioguanine selection (Fig. 7A). We recovered tumor cell colonies from the bone marrow in 3 of 5 animals inoculated with control 4T1 cells (Fig. 7B). By contrast, colonies were recovered from only 1 of 5 mice inoculated with 4T1 cells silenced for miR-10b (Fig. 7B). Similarly, tumor cell colonies were recovered from the lungs in only 2 of 5 mice inoculated with 4T1 cells silenced for miR-10b, whereas tumor cell colonies were recovered from the lungs of 4 of 5 mice bearing control 4T1 cells (Fig. 7C). Taken together, these data show that miR-10b contributes to the engraftment of *TWIST1*-expressing breast cancer cells in the bone marrow and lungs.

## Discussion

There are a number of experimental findings providing evidence that aberrant *TWIST1* reactivation in human breast cancer is associated with tumorigenesis and lung metastasis formation.<sup>(7,9,11–13)</sup> The contribution of *TWIST1* in the development of bone metastasis *in vivo* was, however, unknown. In the present study, we demonstrated that *TWIST1* facilitates experimental breast cancer bone metastasis formation. Specifically, skeletal tumor outgrowth and bone destruction in metastatic animals were both markedly increased when *TWIST1* expression in B02 breast cancer cells was turned on by dox withdrawal. In osteolytic lesions, there is a vicious circle whereby metastatic breast cancer cells in the bone marrow stimulate osteoclast-mediated bone destruction, and bone-derived growth factors released from resorbed bone stimulate skeletal tumor outgrowth.<sup>(1)</sup> We showed here that *TWIST1* promoted this vicious circle by enhancing skeletal tumor outgrowth, which in turn stimulated bone destruction. It has been previously reported that *TWIST1* in PC-3 prostate cancer cells promotes PC-3-mediated osteoclast differentiation *in vitro* and stimulates *DKK-1* expression.<sup>(24)</sup> Here, the conditioned medium from B02 cells promoted

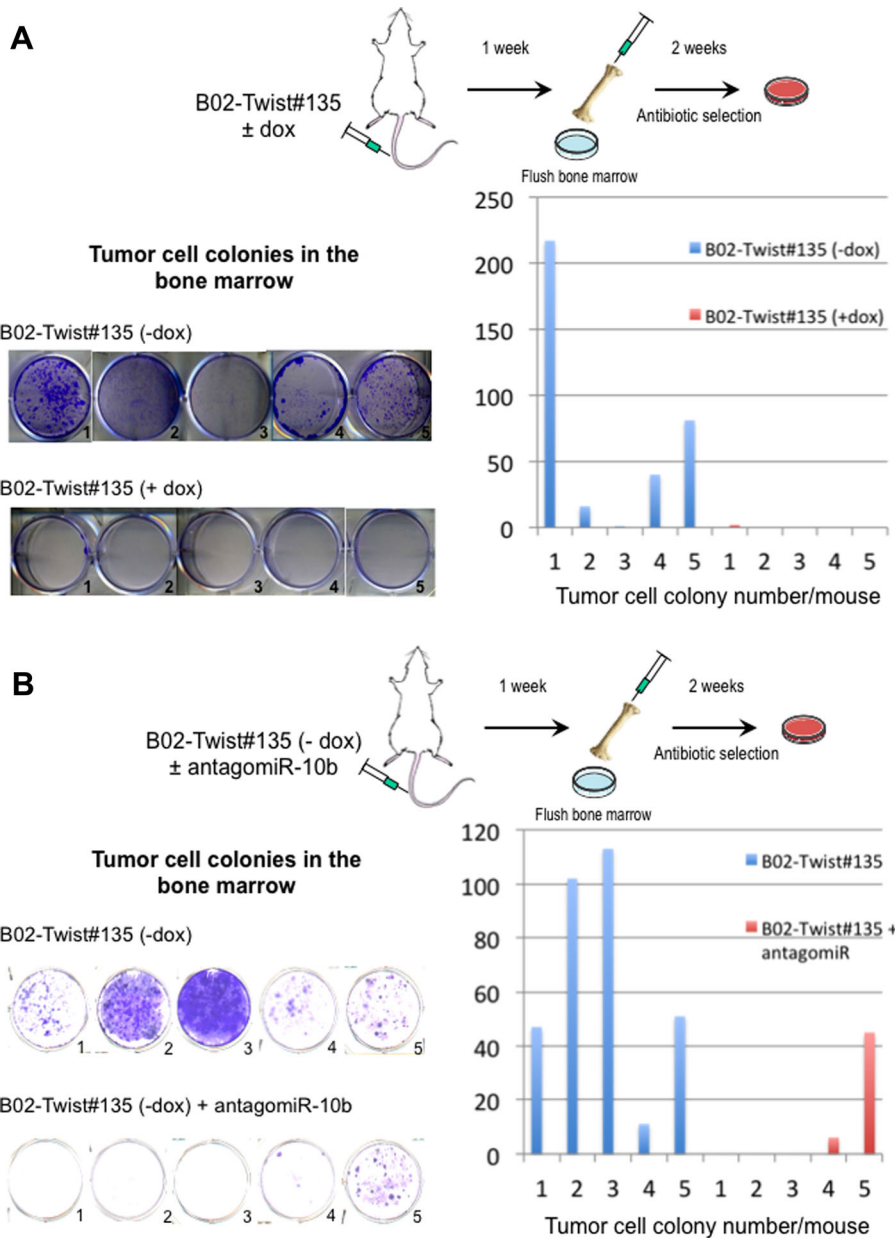


**Fig. 6.** *TWIST1* expression enhanced the presence of B02 breast cancer cells in the bone marrow. (A) Doxycycline (dox)-treated or untreated B02#Twist-135 cells were injected into the tail artery of animals treated with dox or left untreated. *TWIST1* expression in B02#Twist-135 cells was turned off by dox. One week after tumor cell inoculation, the bone marrow was collected from the hind limbs of these animals and placed in culture under antibiotic selection, allowing the selective growth of antibiotic-resistant tumor cells. After 2 weeks in culture, tumor cell colonies recovered from the bone marrow were fixed, stained and counted. Left-hand panels: Each well shows outgrowth of tumor cell colonies from the bone marrow of a single animal. There were 5 mice per group. Right-hand panel: Graph showing the total number of tumor cell colonies formed in the bone marrow from each mouse that received dox or was left untreated. (B) Untreated B02#Twist-135 cells, that were mock-transfected or transfected with antagoniR-10b, were injected into the tail artery of animals. One week after tumor cell inoculation, the bone marrow was collected from the hind limbs of these animals and placed in culture under antibiotic selection. Remaining of the experiment was performed as described in A. Left-hand panels: Each well shows outgrowth of tumor cell colonies from the bone marrow of a single animal. There were 5 mice per group. Right-hand panel: Graph showing the total number of tumor cell colonies formed in the bone marrow from each mouse bearing B02#Twist-135 cells that were mock-transfected or transfected with antagoniR-10b.

osteoclast differentiation in vitro regardless of *TWIST1* expression. Additionally, *DKK-1* was only modestly upregulated in *TWIST1*-expressing breast cancer cells, whereas several other cytokines (MCP-1, GM-CSF, IL-6, IL-8) that stimulate osteoclast differentiation were also produced by these tumor cells

irrespective of *TWIST1*. Yuen and colleagues<sup>(24)</sup> used a murine macrophage cell line, RAW264.7, whereas we gave greater importance to the use of mouse primary bone marrow cells as a model to induce the formation of osteoclasts. The use of different cellular models for osteoclast differentiation could account for

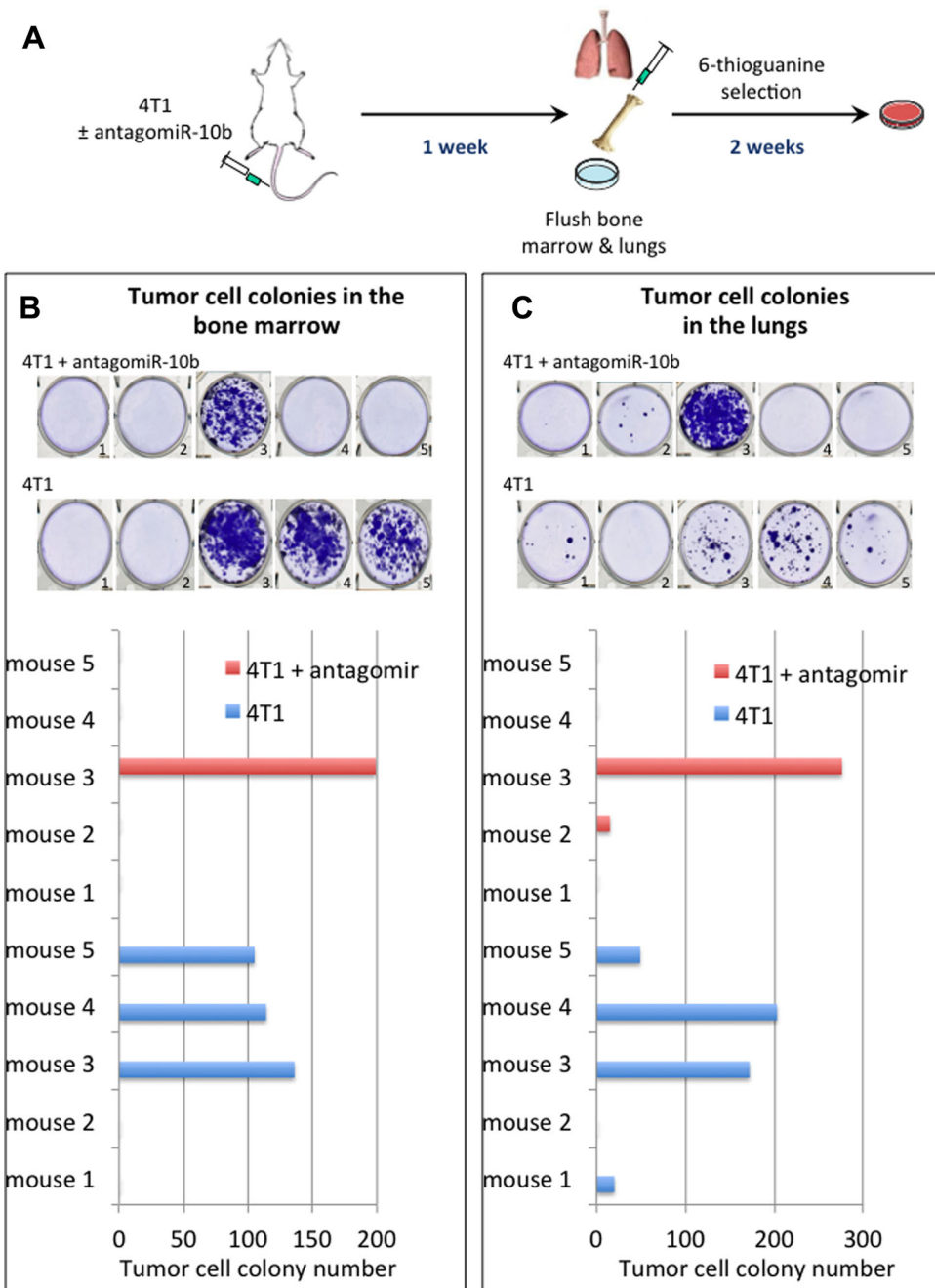


**Fig. 7.** Suppression of miR-10b reduced the presence of 4T1 breast cancer cells in the bone marrow and lungs. (A) 4T1 cells, that were mock-transfected or transfected with antagomir-10b, were injected into the tail artery of animals. One week after tumor cell inoculation, the bone marrow and lungs were collected and cell suspensions were placed in culture under 6-thioguanine selection, allowing the selective growth of antibiotic-resistant tumor cells. After 2 weeks in culture, tumor cell colonies recovered from the bone marrow and lungs were fixed, stained, and counted. (B) Upper panels: Each well shows outgrowth of tumor cell colonies from the bone marrow of a single animal. There were 5 mice per group. Lower panel: Graph showing the total number of tumor cell colonies formed in the bone marrow from each mouse bearing 4T1 cells that were mock-transfected or transfected with antagomir-10b. (C) Same as B for the presence of tumor cell colonies in the lungs.

the discrepancy between the two studies. Although TWIST1 did not enhance the intrinsic ability of B02 cells to produce cytokines that stimulate osteoclast differentiation, we observed a stimulatory effect on osteoclast activity in vitro, as judged by increased Ctsk (Cathepsin K) expression in osteoclasts, further indicating that TWIST1 promoted both skeletal tumor burden and bone

destruction in vivo. The effect of TWIST1 on PC3-induced osteolytic lesions in animals has not yet been investigated, making any additional comparison with our experiments difficult. Such a study would be of interest, as the role of TWIST1 in bone metastasis formation may vary according to the type of cancer.

Having shown that TWIST1 promoted the development of breast cancer osteolytic lesions, we then attempted to determine the specific steps of bone metastasis to which TWIST1 could contribute. Twist1 has been reported as a link between EMT, the intravasation of breast cancer cells in the systemic circulation, and their dissemination to the lungs.<sup>(11)</sup> Our present results establish that TWIST1 promoted breast cancer cell dissemination to the bone (Fig. 3A). TWIST1 expression in B02 cells did not modify the morphological appearance of these already mesenchymal cells and it only modestly affected the expression of major EMT-inducing transcription factors (SNAI1, SNAI2, ZEB1, and ZEB2), indicating that TWIST1 in B02 cells did not contribute to breast cancer bone metastasis formation by promoting an EMT. However, TWIST1 is expressed in disseminated breast cancer cells that persist in the bone marrow after chemotherapy,<sup>(8)</sup> suggesting this transcription factor must have some robust EMT-independent functions that promote the seeding, adaptation, and/or survival of metastatic cells in this bone microenvironment. A current hypothesis gaining ground is that disseminated tumor cells in the bone marrow must acquire bone-like properties to adapt and thrive in the bone microenvironment, a process called osteomimicry.<sup>(1,20)</sup> For example, human bone metastatic breast cancer cells, including MDA-MB-231 and B02 cells, express osteoblast-related factors, such as RUNX2 and CDH-11 (cadherin-11).<sup>(20,26)</sup> However, the expression of RUNX2 and CDH-11 in B02-Twist#135 cells remained unchanged compared with control B02 cells, suggesting that TWIST1 did not affect osteomimicry. Additionally, TWIST1 was not required for the proliferation of B02 cells when grown in culture and as xenografts *in vivo*. TWIST1 did not modulate tumor cell apoptosis either. These results were in agreement with previous findings showing that suppression of *Twist1* does not affect the proliferation of 4T1 breast cancer cells *in vitro* and *in vivo*.<sup>(11)</sup> Moreover, *Twist1* depletion in 4T1 breast cancer cells does not affect cell survival.<sup>(11)</sup> Our data may be explained by the fact that B02 cells (and the MDA-MB-231 parental cell line) carry a KRAS(G13D) mutation that leads to the constitutive phosphorylation of YB-1 and extracellular signal-regulated kinase (ERK)1/2, which in turn endows these tumor cells with a cell growth advantage.<sup>(27,28)</sup> This observation likely explains why TWIST1 in B02 cells did not modulate the activity of YB-1 (Fig. 2B), which is a target gene.<sup>(23)</sup>

Although TWIST1 was dispensable for growth of B02 cells *in vivo*, tumor establishment of TWIST1-expressing B02 cells in the mammary gland of animals was markedly accelerated. It has been previously reported that ectopic TWIST1 expression in MCF-7 breast cancer cells stimulates VEGF production and tumor vascularization, enhancing the establishment of MCF-7/Twist1 tumors in the mammary gland of *nude* mice, when compared with MCF-7/control tumors.<sup>(25)</sup> TWIST1 in B02 cells did not, however, increase the microvessel density of tumor xenografts (Fig. 5B). Indeed, we have previously shown that B02 cells, which do not express TWIST1, produce VEGF levels that are high enough to ensure a correct tumor vascularization.<sup>(16)</sup> Besides accelerating tumor establishment in the mammary gland, our results also showed that TWIST1 markedly enhanced the incidence and number of tumor cell colonies, which were recovered in the bone marrow from animals inoculated with TWIST1-expressing B02 cells. It is possible that TWIST1 promoted the survival of B02 cells in the mammary gland and bone marrow. For example, TWIST1 in MCF7-I4 and MDA-MB-453-I4 breast cancer cells mediates prosurvival and proinvasive functions, at least in part, through the activation of the cell-survival AKT2 kinase.<sup>(29)</sup> However, the

effects of TWIST1 on cell survival are cell-type-specific.<sup>(10,29)</sup> In our study, TWIST1-mediated effects on B02 cells rather resemble those reported on 4T1 and MDA-MB-231 breast cancer cells.<sup>(11,13,30)</sup> For instance, we (this study) and others<sup>(11,13,30)</sup> have shown that TWIST1 endowed B02, MDA-MB-231 and 4T1 cells with higher invasiveness *in vitro*, and that this TWIST1-dependent invasive process was associated with a robust expression of miR-10b, a prometastatic factor. Additionally, we showed that TWIST1 enhanced stemness traits of B02 cells, increasing CD44 expression. Interestingly, CD44 facilitates the arrest of CD44-expressing MDA-MB-231 cells in the bone marrow and the treatment of MDA-MB-231 cells with an anti-CD44 antibody reduces miR-10b production.<sup>(30,31)</sup> Additionally, we showed that the repression of miR-10b in TWIST1-expressing breast cancer cells substantially decreased the incidence and number of tumor cell colonies recovered from the bone marrow and lungs of animals. Hence, our results align with previous studies<sup>(30,31)</sup> and strongly suggest that TWIST1 promotes the seeding and colonization of breast cancer cells in the bone marrow through, at least in part, CD44-dependent and miR-10b-dependent mechanisms.

In summary, we have provided evidence that TWIST1 enhances the presence of breast cancer cells in the bone marrow, which in turn leads to an increase in tumor burden and bone destruction.

## Disclosures

All authors state that they have no conflicts of interest.

## Acknowledgments

PC is supported by INSERM, the University of Lyon and the Seventh Framework Programme (Marie Curie-ITN grant n° 264817; BONE-NET, "European Training Network on Cancer-Induced Bone Disease"). PC and MC also acknowledge the support of the Ligue Nationale contre le Cancer (comité du Rhône), the Fondation de France (grant n°00016390), ARC (grant n°SFI20111203869), and the IFR62 (Lyon, France). AF is a recipient of a fellowship from BONE-NET. AP and SA's team is supported by The Ligue Nationale contre le Cancer as Equipe Labellisée. Additionally, this work was supported by the LabEX DEVweCAN (ANR-10-LABX-61) of Université de Lyon, within the program "Investissements d'Avenir" (ANR-11-IDEX-0007) operated by the French National Research Agency (ANR).

Authors' roles: Study design: MC and PC. Study conduct: MC, AF, and DG. Data collection: MC, AF, EB, and DG. Data analysis: MC and PC. Data interpretation: MC, EB, SA, AP, and PC. Drafting manuscript: MC and PC. Revising manuscript content: AF, DG, EB, SA, and AP. Approving final version of manuscript: MC, AF, DG, EB, SA, AP, and PC. MC and DG take responsibility for the integrity of the data analysis.

## References

1. Weilbaecher KN, Guise TA, McCauley LK. Cancer to bone: a fatal attraction. *Nat Rev Cancer*. 2011;11(6):411–24.
2. Coleman R, Gnant M, Morgan G, Clézardin P. Effects of bone-targeted agents on cancer progression and mortality. *J Natl Cancer Inst*. 2012;104(14):1059–67.
3. Bednarz-Knoll N, Alix-Panabières C, Pantel K, Riethdorf S. Clinical relevance and biology of circulating tumor cells. *Breast Cancer Res*. 2011;13(6):228.

4. Braun S, Vogl FD, Naume B, et al. A pooled analysis of bone marrow micrometastasis in breast cancer. *N Engl J Med.* 2005;353(8):793–802.
5. Baccelli I, Schneeweiss A, Riethdorf S, et al. Identification of a population of blood circulating tumor cells from breast cancer patients that initiates metastasis in a xenograft assay. *Nat Biotechnol.* 2013 Jun;31(6):539–44.
6. Yu M, Bardia A, Wittner BS, et al. Circulating breast tumor cells exhibit dynamic changes in epithelial and mesenchymal composition. *Science.* 2013;339(6119):580–4.
7. Ansieau S, Morel AP, Hinkal G, Bastid J, Puisieux A. TWISTing an embryonic transcription factor into an oncoprotein. *Oncogene.* 2010;29(22):3173–84.
8. Watson MA, Ylagan LR, Trinkaus KM, et al. Isolation and molecular profiling of bone marrow micrometastases identifies TWIST1 as a marker of early tumor relapse in breast cancer patients. *Clin Cancer Res.* 2007;13(17):5001–9.
9. Riaz M, Sieuwerts AM, Look MP, et al. High TWIST1 mRNA expression is associated with poor prognosis in lymph node-negative and estrogen receptor-positive human breast cancer and is co-expressed with stromal as well as ECM related genes. *Breast Cancer Res.* 2012;14(5):R123.
10. Ansieau S, Bastid J, Doreau A, et al. Induction of EMT by twist proteins as a collateral effect of tumor-promoting inactivation of premature senescence. *Cancer Cell.* 2008;14(1):79–89.
11. Yang J, Mani SA, Donaher JL, et al. Twist, a master regulator of morphogenesis, plays an essential role in tumor metastasis. *Cell.* 2004;117(7):927–39.
12. Eckert MA, Lwin TM, Chang AT, et al. Twist1-induced invadopodia formation promotes tumor metastasis. *Cancer Cell.* 2011;19(3):372–86.
13. Ma L, Teruya-Feldstein J, Weinberg RA. Tumour invasion and metastasis initiated by microRNA-10b in breast cancer. *Nature.* 2007;449(7163):682–8.
14. El-Hai CP, Bell GW, Zhang J, et al. Critical role for lysyl oxidase in mesenchymal stem cell-driven breast cancer malignancy. *Proc Natl Acad Sci U S A.* 2012;109(43):17460–5.
15. Peyruchaud O, Winding B, Pécheur I, Serre CM, Delmas P, Clézardin P. Early detection of bone metastases in a murine model using fluorescent human breast cancer cells: application to the use of the bisphosphonate zoledronic acid in the treatment of osteolytic lesions. *J Bone Miner Res.* 2001;16(11):2027–34.
16. Peyruchaud O, Serre CM, NicAmhlaoibh R, Fournier P, Clézardin P. Angiostatin inhibits bone metastasis formation in nude mice through a direct anti-osteoclastic activity. *J Biol Chem.* 2003;278(46):45826–32.
17. Fradet A, Sorel H, Bouazza L, et al. Dual function of ER $\alpha$  in breast cancer and bone metastasis formation: implication of VEGF and osteoprotegerin. *Cancer Res.* 2011;71(17):5728–38.
18. Boucharaba A, Serre CM, Grès S, et al. Platelet-derived lysophosphatidic acid supports the progression of osteolytic bone metastases in breast cancer. *J Clin Invest.* 2004;114(12):1714–25.
19. Fradet A, Sorel H, Depalle B, et al. A new murine model of osteoblastic/osteolytic lesions from human androgen-resistant prostate cancer. *PloS One.* 2013;8(9):e75092.
20. Bellahcène A, Bachelier R, Detry C, Lidereau R, Clézardin P, Castronovo V. Transcriptome analysis reveals an osteoblast-like phenotype for human osteotropic breast cancer cells. *Breast Cancer Res Treat.* 2007;101(2):135–48.
21. Tran DD, Corsa CA, Biswas H, Aft RL, Longmore GD. Temporal and spatial cooperation of Snail1 and Twist1 during epithelial-mesenchymal transition predicts for human breast cancer recurrence. *Mol Cancer Res.* 2011;9(12):1644–57.
22. Casas E, Kim J, Bendesky A, Ohno-Machado L, Wolfe CJ, Yang J. Snail2 is an essential mediator of twist1-induced epithelial-mesenchymal transition and metastasis. *Cancer Res.* 2011;71(1):245–54.
23. Shiota M, Izumi H, Onitsuka T, et al. Twist promotes tumor cell growth through YB-1 expression. *Cancer Res.* 2008;68(1):98–105.
24. Yuen HF, Kwok WK, Chan KK, et al. TWIST modulates prostate cancer cell-mediated bone cell activity and is upregulated by osteogenic induction. *Carcinogenesis.* 2008;29(8):1509–18.
25. Mironchik Y, Winnard PT Jr, Vesuna F, et al. Twist overexpression induces *in vivo* angiogenesis and correlates with chromosomal instability in breast cancer. *Cancer Res.* 2005;65(23):10801–9.
26. Pratap J, Wixted JJ, Gaur T, et al. Runx2 transcriptional activation of Indian Hedgehog and a downstream bone metastatic pathway in breast cancer cells. *Cancer Res.* 2008;68(19):7795–2.
27. Toulany M, Schickfluss TA, Eicheler W, Kehlbach R, Schittek B, Rodemann HP. Impact of oncogenic K-RAS on YB-1 phosphorylation induced by ionizing radiation. *Breast Cancer Res.* 2011;13:R28.
28. Eckert LB, Repasky GA, Ülkü AS, et al. Involvement of Ras activation in human breast cancer cell signaling, invasion, and anoikis. *Cancer Res.* 2004;64:4585–92.
29. Cheng GZ, Zhang W, Wang LH. Regulation of cancer cell survival, migration, and invasion by Twist: AKT2 comes to interplay. *Cancer Res.* 2008;68(4):957–60.
30. Bourguignon LY, Wong G, Earle C, Krueger K, Spevak CC. Hyaluronan-CD44 interaction promotes c-Src-mediated twist signaling, microRNA-10b expression, and RhoA/RhoC up-regulation, leading to Rho-kinase-associated cytoskeleton activation and breast tumor cell invasion. *J Biol Chem.* 2010;285(39):36721–35.
31. Hiraga T, Ito S, Nakamura H. Cancer stem-like cell marker CD44 promotes bone metastases by enhancing tumorigenicity, cell motility and hyaluronan production. *Cancer Res.* 2013;73(13):4112–22.